

REPORT DOCUMENTATION PAGE

Form Approved
OMB No. 0704-0188

Public reporting burden for this collection of information is estimated to average 1 hour per response, including the time for reviewing instructions, searching existing data sources, gathering and maintaining the data needed, and completing and reviewing this collection of information. Send comments regarding this burden estimate or any other aspect of this collection of information, including suggestions for reducing this burden to Department of Defense, Washington Headquarters Services, Directorate for Information Operations and Reports (0704-0188), 1215 Jefferson Davis Highway, Suite 1204, Arlington, VA 22202-4302. Respondents should be aware that notwithstanding any other provision of law, no person shall be subject to any penalty for failing to comply with a collection of information if it does not display a currently valid OMB control number. PLEASE DO NOT RETURN YOUR FORM TO THE ABOVE ADDRESS.

1. REPORT DATE (DD-MM-YYYY)

2. REPORT TYPE

Technical Paper

3. DATES COVERED (From - To)

4. TITLE AND SUBTITLE

5a. CONTRACT NUMBER

5b. GRANT NUMBER

5c. PROGRAM ELEMENT NUMBER

62500F

6. AUTHOR(S)

5d. PROJECT NUMBER

2308

5e. TASK NUMBER

M4S7

5f. WORK UNIT NUMBER

345382

7. PERFORMING ORGANIZATION NAME(S) AND ADDRESS(ES)

8. PERFORMING ORGANIZATION
REPORT

9. SPONSORING / MONITORING AGENCY NAME(S) AND ADDRESS(ES)

Air Force Research Laboratory (AFMC)
AFRL/PRS
5 Pollux Drive.
Edwards AFB CA 93524-7048

10. SPONSOR/MONITOR'S
ACRONYM(S)

11. SPONSOR/MONITOR'S
NUMBER(S)

12. DISTRIBUTION / AVAILABILITY STATEMENT

Approved for public release; distribution unlimited.

13. SUPPLEMENTARY NOTES

See attached 13 papers, all with the information on this page.

14. ABSTRACT

15. SUBJECT TERMS

16. SECURITY CLASSIFICATION OF:

a. REPORT

Unclassified

b. ABSTRACT

Unclassified

c. THIS PAGE

Unclassified

17. LIMITATION
OF ABSTRACT

A

18. NUMBER
OF PAGES

19a. NAME OF RESPONSIBLE
PERSON

Kenette Gfeller

19b. TELEPHONE NUMBER
(include area code)

(661) 275-5016



AIAA 94-3337

**A Comparison of Theory and
Measurements in the Anode Region of a
Self-Field Cylindrical MPD Thruster**

**D.L. Tilley, S. Castillo
Phillips Laboratory
Edwards A.F.B., CA 93524**

**M.S. Jolly, E. Niewood, M. Martinez-Sanchez
Massachusetts Institute of Technology
Cambridge, MA 02139**

**30th AIAA/ASME/SAE/ASEE Joint
Propulsion Conference
June 27-29, 1994 / Indianapolis, IN**

A Comparison of Theory and Measurements in the Anode Region of a Self-Field Cylindrical MPD Thruster

D.L. Tilley[‡], S. Castillo[†]
Phillips Laboratory
Edwards A.F.B., CA 93524

M.S. Jolly*, E. Niewood*, M. Martinez-Sanchez**
Massachusetts Institute of Technology
Cambridge, MA 02139

20050815 030

[‡] Research Engineer, Electric Propulsion Laboratory, Member AIAA
[†] Capt USAF, Electric Propulsion Laboratory
* Graduate Student, M.I.T., Space Power and Propulsion Laboratory, Member AIAA
** Professor, M.I.T., Department of Aeronautics and Astronautics, Member AIAA

Abstract

The need to validate and improve numerical models of the MPD thruster flow, using detailed comparisons with experimentally determined plasma properties, is essential in the effort to improve MPD thruster efficiency. This research represents an attempt to experimentally identify trends, in the variation of plasma properties inside of a self-field MPD thruster, which could be meaningfully compared with numerical results. Experimental results, consistent with the numerical model in trend, show an axial variation of the electron temperature along the anode which exhibits a very distinctive double-peaked profile. Experimental axial profiles of the electron number density and current density were also consistent with the numerical model in trend. Such evidence, along with results of the numerical model, suggest that an oblique shock is present near the inlet, and is required to establish the radial pressure gradient so prevalent in the MPD thruster. This work marks one of the first non-trivial, successful comparisons between a numerical model and experimentally determined plasma properties inside the MPD thruster.

I. Introduction

The magnetoplasmadynamic (MPD) thruster is a space propulsion device with the potential to significantly enhance the payload mass delivered to GEO and/or greatly reduce launch costs by enabling launch vehicle downsizing. A recent study has shown that the MPD thruster, due to its higher specific impulse, is capable of providing the above benefits in excess of those provided

by the hydrogen arcjet, with only a small increase in transfer time[1]. The MPD thruster operates by using the Lorentz force to accelerate a plasma to exhaust velocities typically in the 10-50 km/sec range. Unfortunately, two issues must be resolved to actualize such benefits: thruster efficiency and lifetime. The MPD thruster's insistence on operating inefficiently has prohibited its development for use on spacecraft, and has even stunted current MPD thruster R&D efforts in favor of more promising plasma thrusters. The thruster efficiency issue is the focus of this work.

Faced with the problem of low thruster efficiency, MPD thruster research activities have emphasized the investigation of various loss mechanisms in the thruster[2,3]. As part of this focus on loss mechanisms, there has been a substantial increase in the development of numerical codes to investigate the flow physics inside of a self-field thruster. As discussed in a 1991 review, only recently has it been conceivable to directly compare numerical models with experiment[4].

Initially, comparisons of numerically calculated thrust versus terminal current curves compared quite well to experimentally determined curves for self-field MPD thrusters[4,5]. This success came as no surprise, at least in the electromagnetic regime of self-field MPD thruster operation, because the electromagnetic thrust is essentially independent of propellant species and the current density distribution inside of the thruster, as noted in the derivation of the Maecker thrust law[6]. Model comparisons with experimentally determined current contours inside the thruster have also been fairly successful qualitatively and somewhat successful quantitatively[4,7-11]. In the self-field MPD thruster, these comparisons are more relevant to the specific impulse of the thruster, and do not directly address the efficiency problem. It is interesting to note the experimental observations of Turchi, et al.[12], who

This paper is declared a work of the U.S. Government and is not subject to copyright protection in the United States.

noticed that the current contours inside the MPD thruster can be drastically altered by simply changing the flow injection scheme, and that such a change had absolutely no effect on the terminal voltage, and most likely, no effect on the thruster efficiency.

The prediction of the terminal voltage is more relevant to the efficiency problem, because the identification of any method to reduce the thruster voltage (for a given current and mass flow rate) is equivalent to increasing the efficiency of a self-field MPD thruster. Until recently, numerical models had shown little progress at predicting the terminal voltage. Among all of the models, the predicted voltages were universally lower than their experimental counterparts. To investigate this deficiency, researchers have focused on such loss mechanisms as microturbulence effects[10], viscous and diffusive effects[13], and the Hall effect[11,14] on thruster operation. Such efforts have been fruitful, especially the work investigating the Hall effect on the anode fall voltage[11,14]. In that work, terminal voltages predicted by a numerical model, which included the Hall effect on the voltage drop near the anode, compared very well with experiment in both magnitude and trend.

Comparisons of numerical results with terminal and thrust measurements are not enough to validate and improve numerical models[3]. Research efforts are now shifting towards the detailed comparison of numerical results with experimentally determined plasma properties in the MPD thruster interior[15,16]. Trivial comparisons, of trend and magnitude, are easily made with the most rudimentary models, such as the electron density variation with radius, or the peak in electron temperature off the cathode tip. Prior to this investigation, there has been only one non-trivial, satisfying comparison between numerical model and measurements taken inside the MPD thruster (a comparison of Niewood's numerical model[11] to floating voltage measurements[17] at a single location near the anode at various thruster currents).

As models become increasingly more powerful and predictive, the move to the model validation phase will probably be hindered by the lack of high-fidelity plasma property data taken inside the MPD thruster. Arguably the most extensive study of internal plasma properties, that of Tahara, et al.[18], is of limited use in the further refinement of present-day models because most of the experimentally observed trends are dominated by the error in the experimental techniques. These techniques, almost exclusively Langmuir probes, magnetic field probes and emission spectroscopy[3], have been (and still are) instrumental in the investigation of the plasma physics associated with the MPD thruster. However, plasma property data, internal to the MPD thruster, that can be meaningfully compared with numerical models are practically non-existent.

The objective of this research was to attempt to experimentally identify trends, in the variation of plasma properties inside of the MPD thruster, which could be meaningfully compared with numerical results. In particular, for this study, the numerical results of Niewood[11] were used for comparison to experimental results. The approach was to investigate the axial variation of plasma properties in the anode region of a

self-field cylindrical MPD thruster. A self-field cylindrical MPD thruster was used because this configuration is conducive to comparisons with numerical models. Probe diagnostics were utilized because of their ease of use, and the presumption that the systematic error associated with the Langmuir probe was acceptable in the anode region. Finally, the anode region was chosen because it is very relevant to the thruster efficiency problem[11,14,19], and because this region was the focus of the modeling effort of Niewood[11]. Fortunately, and almost serendipitously, the above approach was successful in identifying clear trends in the axial variation of plasma properties along the anode that were consistent with the numerical model.

II. Experimental Apparatus

Experiments were performed with a cylindrical self-field MPD thruster operated in a quasi-steady mode (1-2 msec pulse duration) at the Electric Propulsion Laboratory at the Phillips Laboratory at Edwards AFB, CA. A more complete description of the facility, MPD thruster, and diagnostics used in this research can be found in reference 15, 20, and 21.

Facility

The vacuum chamber, 2.4 m in diameter and 3.6 m in length, was pumped by two 25 cm (10 inch) diffusion pumps to vacuum pressures in the low 10^{-4} torr range, which was the vacuum pressure prior to firing the thruster. Once ignited, typically by a 1 kV pulse, the thruster was powered by a 20 kJ, 800 V maximum pulsed forming network (PFN).

To ensure sufficiently low vacuum during thruster operation, the propellant to the thruster was supplied in a pulsed manner (typical pulse length ~60-80 msec). A piezoelectric pressure transducer was used to monitor the gas pulse, and to verify that the thruster was ignited during steady flow. The uncertainty in the mass flow rate, which was calibrated in situ before each series of tests, was less than 2% (due primarily to variations in the plenum pressure). Research grade argon was the propellant in all testing.

To investigate the effect of the residual vacuum on thruster operation, the voltage to the thruster was measured, at a fixed PFN charging voltage, as the timing between the gas pulse initiation and the ignition of the thruster was varied. The resulting data showed that when the time delay was too short, the voltage increased, and voltage oscillations were observed (characteristic of thruster operation at insufficient mass flow). When the time delay was too long, the thruster voltage gradually decreased, as the entrainment of residual gas began to affect thruster operation. In these experiments, the time delay was fixed in between the above extremes, where the terminal voltage was observed to be independent of the time delay.

MPD Thruster

The cylindrical MPD thruster used in these tests was identical to that used previously at the Phillips Laboratory[20,21]. The copper anode was 10.16 cm OD,

7.62 cm ID and 4.20 cm long (from the boron nitride injection plate), and the thoriated tungsten cathode was 1.27 cm in diameter and 2.3 cm long. Propellant was injected at the back of the thrust chamber, through a boron nitride injection plate, via a series of 16 - 0.32 cm diameter injection holes (8 at a radius of 1.6 cm and 8 at 2.5 cm) and through an annulus with an outer radius of 0.95 cm and inner radius of 0.64 cm at the base of the cathode.

Shown in Fig. 1 is the voltage-current characteristic of the thruster at 0.5 g/sec of argon. All measurements reported in this paper were obtained at a mass flow rate of 0.5 g/sec and at currents below the onset current of 5.6 kA. The voltage of the thruster was measured with the help of a Tektronix 1000:1 voltage probe ($\pm 5\%$), and the current with a Pearson Electronics current monitor (Model No. 301X, 3%/msec droop). The uncertainties in the voltage and current were dominated by shot-to-shot variation (at low currents) and either high-frequency fluctuations or error introduced because the waveform was not quite a flat-top profile (at high currents). As seen previously in this thruster[20,21], onset occurs (based on the 10% peak-to-peak voltage fluctuation criterion) at a relatively low current because most of the propellant is injected through the cathode annulus.

Diagnostics

The measurements reported in this paper are only a small subset of a large data base of internal measurements taken in this MPD thruster. An induction probe was used to measure the magnetic field, and via Maxwell's equations, derive the current density. A triple Langmuir probe[22] was used to obtain the electron temperature, T_e , and electron number density, n_e . A floating probe, along with the triple probe measurements, was used to measure the plasma potential and anode fall voltage. No plasma potential or anode fall data will be reported in this paper; consult reference 15 for further details on these and other measurements.

The induction probe consisted of a 75 turn coil (1.6 mm in diameter, 1.6 mm long) placed in a 4 mm OD quartz tube[15]. The coil was oriented to measure the azimuthal magnetic field, which is the only component in a self-field MPD thruster. Since the induction probe is responsive to dB/dt only, an integrator was employed to obtain the time history of the magnetic field.

The induction probe/integrator system was calibrated by first placing the coil at the largest radius and as far into the thrust chamber as possible. Then by firing the thruster, the magnetic field is calculated by Ampere's law (assuming that the total thruster current is enclosed by the coil, $B = \mu_0 I / 2\pi r$), and correlated with the voltage from the induction probe/integrator system. After firing the thruster at many different currents, a least-squares fit is used to determine the proportionality factor between the voltage and magnetic field. The uncertainty in the magnetic field measurements was dominated by shot-to-shot variation (~ 10 -20%).

A spatial map of the magnetic field inside the MPD thruster was obtained at two operating conditions

(4.4 and 4.8 kA). At each location, the magnetic field was taken to be the average of the measurements corresponding to three firings of the thruster. From the magnetic field map, and Ampere's law ($J_{enc} = 2\pi r B / \mu_0$), an enclosed-current contour map is constructed. The contour map of the enclosed current is then fitted with a 3rd order polynomial surface fit; this surface fit is used to interpret the triple probe measurements.

The triple probe consisted of three cylindrical electrodes (radius=0.063 mm, length=5.2 mm) spaced 1.7 mm apart, aligned with the thruster axis, and configured such that all electrodes were approximately at the same radius from the thruster centerline. With these dimensions, and configuration, the following effects can be neglected: collisional effects, magnetic field effects, electrode end effects, sheath interactions between the electrodes, and gradient effects. Throughout testing, the Langmuir probe was ion bombardment cleaned by establishing a glow discharge between the probe and the thruster anode. This cleaning was performed every 10 shots, which was chosen as a compromise between the need to eliminate contamination effects (cleaning is desired after every measurement) and time constraints. The probe voltage and current, used to calculate T_e and n_e , were taken as the average of three shots. As with the floating probe, triple probe measurements were taken at eight current levels, ranging from 2.2 to 5.3 kA, and 12 axial locations along the anode. In addition, radial profiles at three axial locations were obtained inside of the thruster at 4.4 and 4.8 kA.

The electron temperature and number density were calculated with equations 12 and 18 of reference 22 assuming $T_i = T_e$ and singly ionized argon ions. These expressions were derived from Laframboise's exact calculations for the ion saturation current to a cylinder[23]. A unique feature of the error estimates in this paper is that the values for many of the unknown parameters, used to bound the error, were taken from the calculations of Niewood's model[11]. The model results for the anode region suggest that the value of $T_i/Z_i T_e$ was bounded between 1/3 and 2, and the component of the ion flow perpendicular to the triple probe is negligible compared to the ion thermal velocity. This last finding, which is not valid in most regions of the thruster, significantly reduces the error associated with triple probe measurements[19,22,24]. Another source of error is the unknown ionization state of the plasma. Since doubly ionized argon ions are common in MPD thrusters, the uncertainty in electron number density due to unknown ionization state is accounted for by equation 24 of reference 22 (the number fraction of doubly ionized argon is assumed to be bounded by 0 and 0.5[22]). With the above bounds, the uncertainty in electron number density was dominated by the uncertainty of these parameters. The random error associated with shot-to-shot variation (10-15%) was small compared to the above systematic error. Alternatively, the systematic error associated with electron temperature (due primarily to the electron drift perpendicular to the probe) was small compared to the random error ($\pm 10\%$). Finally, the uncertainty in axial location was taken as one half of the probe length.

III. Experimental Results

One of the more intriguing results of this research is presented in Fig. 2. Shown is the electron temperature, 1.4 mm from the anode, plotted as a function of axial position for the MPD thruster operating at 4.4 kA. Accounting for measurement error, it is clear that the electron temperature exhibits a double-peaked axial profile, with the upstream peak located at 1.2 cm and the downstream peak at 3.4 cm. This phenomenon was observed at all thruster currents examined in this study, as low as 2.2 kA and as high as 5.3 kA[15], with the peaks in the roughly the same locations. To the author's knowledge, this is the first observation of such phenomena in the MPD thruster.

To help explain this phenomenon, and to investigate its implications, the numerical results of Niewood[11] were consulted. The thruster geometry used in this theoretical study is shown in Fig. 3, and is representative of the Constant Area Channel (CAC) thruster used in previous testing[17,25]. As the name implies, the thruster has a cylindrical geometry, is 11 cm in length, and has a cathode and anode radius of 5.2 cm and 7.2 cm respectively. In the model, the CAC thruster is assumed to be operating on argon, consistent with the experimental work of this paper. The three-fluid, two-temperature, 2-D axisymmetric numerical code is one of the most advanced developed for the MPD thruster, and includes many physical processes[11,14]. Most notable of the included physics is the Hall effect, finite-rate ionization/recombination kinetics, and a model for the anode fall voltage.

The axial profile of the electron temperature predicted by the model, in the CAC thruster at a distance of 1.6 mm from the anode, is shown in Fig. 4 (Fig. 7-2 of reference 11). Although the operating condition (39.0 kA, 4 g/sec argon) and geometry of the CAC thruster are quite different from that used in this experimental study, the magnitude and double-peaked trend is very similar to the experimental data shown in Fig. 2. Also note that the double-peaked T_e profile was observed in one other numerical modeling effort[26], as will be discussed later.

To understand this behavior, it is helpful to qualitatively examine the electron energy equation. Assuming that ohmic dissipation is balanced by collisional transfer between electrons and ions, the following relation can be derived:

$$\frac{3k(T_e - T_i)}{M_i} = \left(\frac{j}{en_e} \right)^2 \quad (1)$$

where j is the current density, e is the electron charge, k is Boltzman's constant, and M_i is the ion mass. Assuming T_i is relatively constant, this expression states that T_e is larger in regions of high current density and low electron density. Although this expression neglects such effects as heat conduction and convection, pressure work, viscous dissipation, and the transfer of electron energy to and from

the internal modes of the ions, it is expected that these terms will be second order in this simple analysis.

Shown in Fig. 5 is an experimentally determined contour plot of the enclosed current in the MPD thruster operating at 4.4 kA. The characteristic that most of the current is emitted from the base of the cathode and attaches at the downstream end of the anode has been observed in this thruster previously[21]. Another map, taken at 4.8 kA was also very similar to Fig. 5. Fig. 5 shows that the current density, in the region of the downstream T_e peak ($z=3.4$ cm), is very large and in fact peaks in this region (j is proportional to the density of the contour lines). Eq. 1 suggests, due to large ohmic heating, that this local maximum in current density is responsible for the peak in T_e . Such a correlation of j with T_e has been observed experimentally[18,19] and computationally[26,27] many times at the cathode tip and anode. The downstream T_e peak in the model, shown in Fig. 4, also corresponds to the large current density at the downstream edge of the anode (see Fig. 6-2 of reference 11).

The upstream T_e peak, for both the model and this experimental work, is in a region of low current density. Thus, from equation 1, it is presumed that the electron density is low in this region. This is indeed the case for both the model and experiment. Shown in Fig. 6 are the numerical results for the axial variation of electron number density, at a distance of 1.6 mm from the anode, as a function of thruster current. Clearly, at 39 kA, a minimum in electron number density is seen 2 to 4 cm downstream from the backplate. In Fig. 7, the measured axial profile of electron number density at 4.4 kA also exhibits a valley at the same location of the upstream T_e peak in Fig. 2. Again, this behavior was observed at thruster currents ranging from 2.2 to 5.3 kA[15]. As expected, the magnitudes of the electron number densities in Fig's 6 and 7 do not compare, because of the significantly different mass flow rates in the CAC thruster (4 g/sec) and the MPD thruster used in these experiments (0.5 g/sec).

Before moving on, two points will be made about Fig. 7. First, although the random error associated with the electron number density measurements is non-negligible, the majority of the error is systematic due to unknown T_i and species concentrations. The upper bound on n_e was calculated assuming $T_i/Z_i T_e = 1/3$ and singly ionized argon ions only. The lower bound was estimated assuming $T_i/Z_i T_e = 2$ and a number fraction of doubly ionized argon ions of 0.5. Since these parameters vary considerably along the anode (see Fig. 4 for example), it may not be valid to assume that the actual axial profile is simply a shift in the vertical direction of the experimentally determined profile. Secondly, it was mentioned earlier that a double-peaked T_e profile along the anode was observed numerically by Sleziona, et al.[26]. Upon examining their results, it is believed that both peaks are due to high current densities, and not from a density minimum.

In Fig. 6 the numerical model indicates that the density minimum is persistent over a large range of thruster currents. As noted above, this was also the case experimentally. In addition, Fig. 6 indicates that the

electron density minimum shifts downstream as the thruster current is increased (for a given mass flow rate). Again, there is consistency between the model and experiment. In Fig. 8, it is seen that at 2.6 kA, the density minimum is located at 1.2 ± 0.26 cm downstream of the backplate, while at 5.1 kA, it has moved downstream to $z = 1.8 \pm 0.26$ cm. As seen in Fig. 7, at 4.4 kA the density minimum is located between these two extremes. Also shown in Fig. 8, denoted by the open symbols, are the locations of the electron temperature peaks.

With such agreement between experiment and numerical model, a logical question now arises from these results: why is there a density minimum at the anode, near the inlet of the MPD thruster? The answer to this question is found by further examination of the numerical results of Niewood. Shown in Fig 9 is a contour plot of the radial velocity inside of the CAC thruster. This plot shows that large negative radial velocities occur at the inlet of the thruster, and near the region of the upstream T_e peak. The cause of this inward flow is that as soon as the propellant enters the thrust chamber, it is accelerated towards the cathode by the Lorentz force in the negative r -direction. Even though the r -component of the Lorentz force is much smaller than the axial component, it is initially unbalanced due to the lack of a radial pressure gradient at the inlet of the thruster. The rush of plasma towards the cathode reduces the electron number density near the anode.

Shown in Fig 10 are the streamlines and pressure contours in the first 3 cm downstream of the inlet. This figure shows that as the flow approaches the cathode, it is turned axially by what appears to be an oblique shock. The oblique shock, which is diffused in part by viscous effects and possibly by numerical smearing, can be seen as the pressure rise in lower right-hand side of Fig. 10. Consequently, the density minimum, and thus the upstream T_e peak, is formed by the initial acceleration of the plasma towards the cathode at the inlet and the contact of the oblique shock to the anode. Only, an advanced 2-D numerical code, such as that of Niewood, is capable of explaining such phenomenon.

In summary, near the inlet of the thrust chamber, an oblique shock is required to establish the radial pressure gradient inside the MPD thruster. Considering the differences in geometries of the CAC thruster and the experimental MPD thruster, and the wide span in operating conditions investigated in this study, it appears that this phenomenon may be characteristic of all self-field MPD thrusters.

IV. Conclusions

The objective of this research was to experimentally identify trends, in the variation of plasma properties inside of a self-field MPD thruster, which could be meaningfully compared with numerical results. The approach to this objective was to investigate the axial variation of plasma properties in the anode region and compare them to the numerical results of an advanced numerical model developed at M.I.T. Experimental

results showed that the axial variation of the electron temperature along the anode exhibits a very distinctive double-peaked profile. This unique feature was observed at all thruster operating conditions (2.2 - 5.3 kA, 0.5 g/sec) examined in this study, and was also predicted by the model. Experimental axial profiles of the electron number density (showing a minimum at the location of the upstream T_e peak) and current densities (showing a maximum at the location of the downstream T_e peak) are also consistent with the numerical model in trend. As observed in previous studies, the downstream peak is produced by large ohmic heating from the high current density at the downstream edge of the anode. The upstream T_e peak is a consequence of an electron density minimum created by the inlet fluid dynamics of the thruster.

With increased confidence in the numerical model, it was further used to investigate the implications of such an upstream T_e peak. Based on numerical results, it is created in part by the unbalanced radial Lorentz force at the inlet of the thruster, and the subsequent oblique shock which is required to establish the radial pressure gradient inside the MPD thruster. Due to the resilience of this phenomenon to thruster operating conditions, this internal flow structure at the inlet may be a characteristic of all MPD thrusters.

Although the agreement between experiment and theory in all of the above profiles is in trend only, it marks one of the first non-trivial, successful comparisons between numerical model and experimentally determined plasma properties inside of the MPD thruster.

Acknowledgments

The authors would like to thank Jeff Pobst, Phillips Laboratory, for preparing Fig. 5.

References

- 1) Myers, R.M., Domonkos, M., Gilland, J.H., "Low Power Pulsed MPD Thruster System Analysis and Applications, AIAA Paper No. 93-2391, 1993.
- 2) Myers, R.M., ed., "Magnetoplasma-dynamic Thruster Workshop", NASA CP-10084, 1991.
- 3) Myers, R.M., ed., "Second Magnetoplasma-dynamic Thruster Workshop", NASA CP-10109, 1992.
- 4) Myers, R.M., Mantenieks, M.A., LaPointe, M.R., "MPD Thruster Technology", AIAA Paper No. 91-3568, 1991.
- 5) LaPointe, M.R., "Numerical Simulation of Cylindrical, Self-Field MPD Thrusters with Multiple Propellants", IEPC Paper No. 93-074, 1993.
- 6) Maecker, H., "Plasma Jets in Arcs in a Process of Self-Induced Magnetic Compression" (in German), Z. Phys., Vol. 141, pp. 198-216, 1955.

- 7) Slezione, P.C., Auweter-Kurtz, M., Schrade, H.O., "Numerical Codes for Cylindrical MPD Thrusters", IEPC Paper No. 88-038, 1988.
- 8) Slezione, P.C., Auweter-Kurtz, M., Schrade, H.O., "Numerical Evaluation of MPD Thrusters", AIAA Paper No. 90-2602, 1990.
- 9) LaPointe, M.R., "Numerical Simulation of Self-Field MPD Thrusters", AIAA Paper No. 91-2341, 1991.
- 10) Caldo, G., Choueiri, E.Y., Kelly, A.J., Jahn, R.G., "Numerical Fluid Simulation of an MPD Thruster with Real Geometry", IEPC Paper No. 93-072, 1993.
- 11) Niewood, E.H., "An Explanation for Anode Voltage Drops in an MPD Thruster", Ph.D. Thesis, Massachusetts Institute of Technology, June 1993. See also AIAA Paper No. 93-2104, 1993.
- 12) Turchi, P.J., Davis, J.F., Roderick, N., "MPD Arcjet Thrust Chamber Flow Studies", AIAA Paper No. 90-2664, 1990.
- 13) Miller, S. and Martinez-Sanchez, M., "Viscous and Diffusive Effects in Electrothermal and MPD Arcjet Thrusters", IEPC Paper No. 91-060, 1991.
- 14) Niewood, E.H. and Martinez-Sanchez, M., "The Hall Effect in a Numerical Model of MPD Thrusters", IEPC Paper No. 91-099, 1991.
- 15) Jolly, M.S., "A Voltage Drop Study in a Megawatt Level Quasi-Steady Magnetoplasma Dynamic Thruster Via Probe Diagnostics", M.S. Thesis, Massachusetts Institute of Technology, June 1993.
- 16) Slezione, P.C., et al., "Calculation of a Nozzle Type MPD Thruster and Comparison with Measurements", IEPC Paper No. 93-191, 1993.
- 17) Heimerdinger, D.J. and Martinez-Sanchez, M., "Design and Performance of an Annular Magnetoplasma Dynamic Thruster", J. Propulsion & Power, Vol. 7, No. 6, pp. 975-980, 1991.
- 18) Tahara, H., Yasui, H., Kagaya, Y., Yoshikawa, T., "Experimental and Theoretical Researches on Arc Structure in a Self-Field Thruster", AIAA Paper No. 87-1093, 1987.
- 19) Gallimore, A.D., "Anode Power Deposition in Coaxial MPD Thrusters", Ph.D. Thesis, Princeton University, October 1992.
- 20) Castillo, S. and Tilley, D.L., "The Air Force Phillips Laboratory Multimegawatt Quasi-Steady MPD Thruster Facility", AIAA Paper No. 92-3158, 1992.
- 21) Bowman, E. and Tilley, D.L., "Microinstabilities in High-Power MPD Systems: Preliminary Diagnostics", IEPC Paper No. 93-125, 1993.
- 22) Tilley, D.L., Kelly, A.J., Jahn, R.G., "The Application of the Triple Probe Method to MPD Thruster Plumes", AIAA Paper No. 90-2667, 1990.
- 23) Laframboise, J., "Theory of Cylindrical and Spherical Langmuir Probes in a Collisionless Plasma at Rest", ITIAS Report No. 100, 1966.
- 24) Tilley, D.L., Gallimore, A.D., Kelly, A.J., Jahn, R.G., "The Adverse Effect of Perpendicular Ion Drift Flow on Cylindrical Triple Probe Electron Temperature Measurements", Rev. Sci. Instrum., Vol. 65, pp. 678-681, 1994.
- 25) Kilfoyle, D.B., Martinez-Sanchez, M., Heimerdinger, D.J., Sheppard, E.J., "Spectroscopic Investigation of the Exit Plane of an MPD Thruster", IEPC Paper No. 88-027, 1988.
- 26) Slezione, P.C., Auweter-Kurtz, M., Schrade, H.O., "Numerical Calculation of a Cylindrical MPD Thruster", IEPC Paper No. 93-066, 1993.
- 27) Slezione, P.C., Auweter-Kurtz, M., Schrade, H.O., Wegmann, T., "Comparisons of Numerical and Experimental Investigations of Nozzle Type MPD Accelerators", AIAA Paper No. 90-2663, 1990.

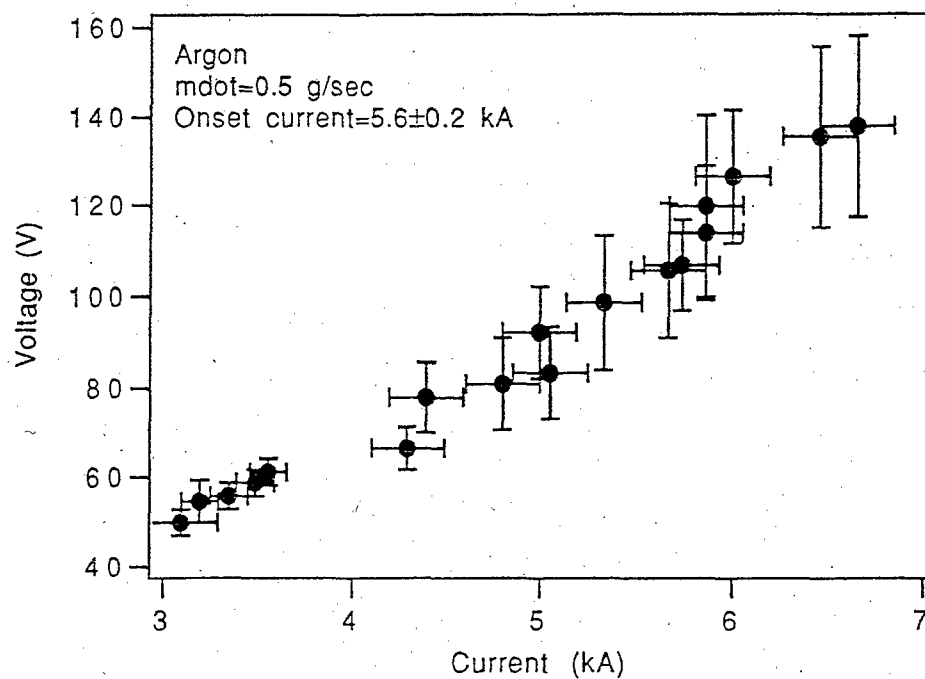


Fig. 1: The voltage-current characteristic of the experimental MPD thruster.

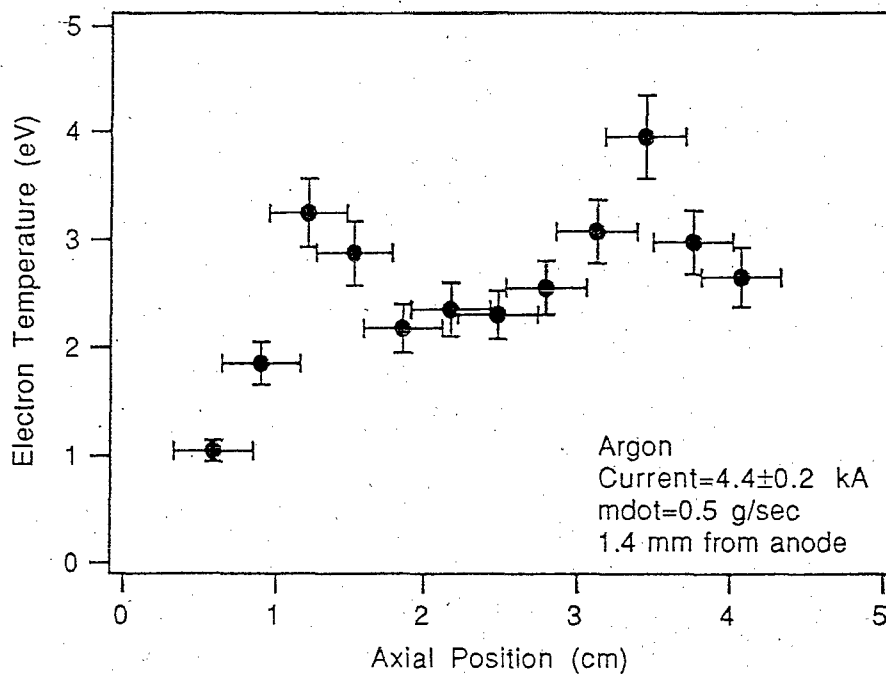


Fig. 2: An axial profile of the measured electron temperature near the anode.

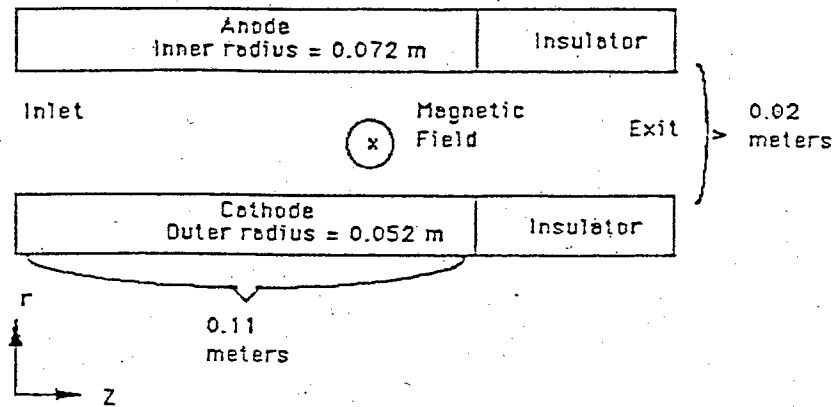


Fig. 3: The geometry of the MPD thruster used in Niewood's[11] numerical model.

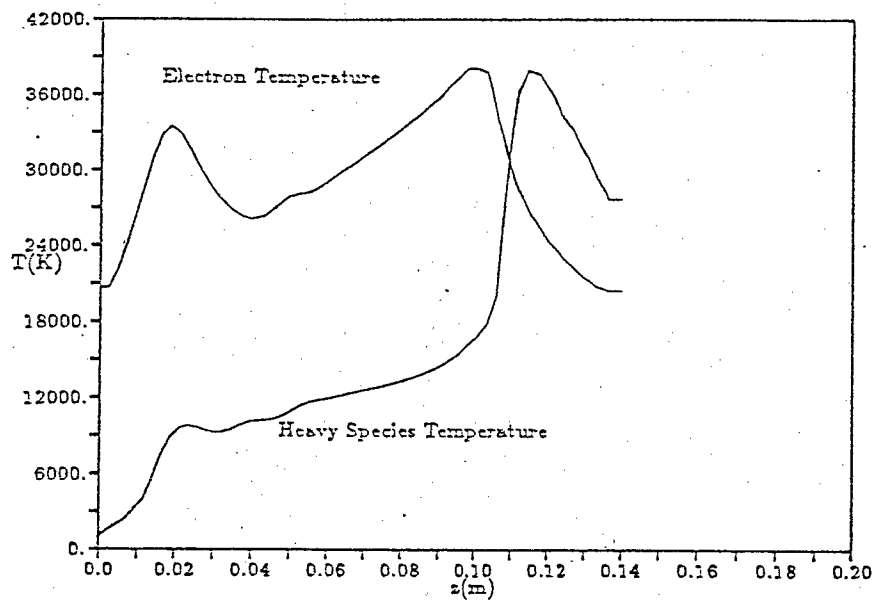


Fig. 4: Model predictions for the species temperatures, 1.6 mm from the anode, for the CAC thruster operating at 39 kA, 4 g/sec argon.

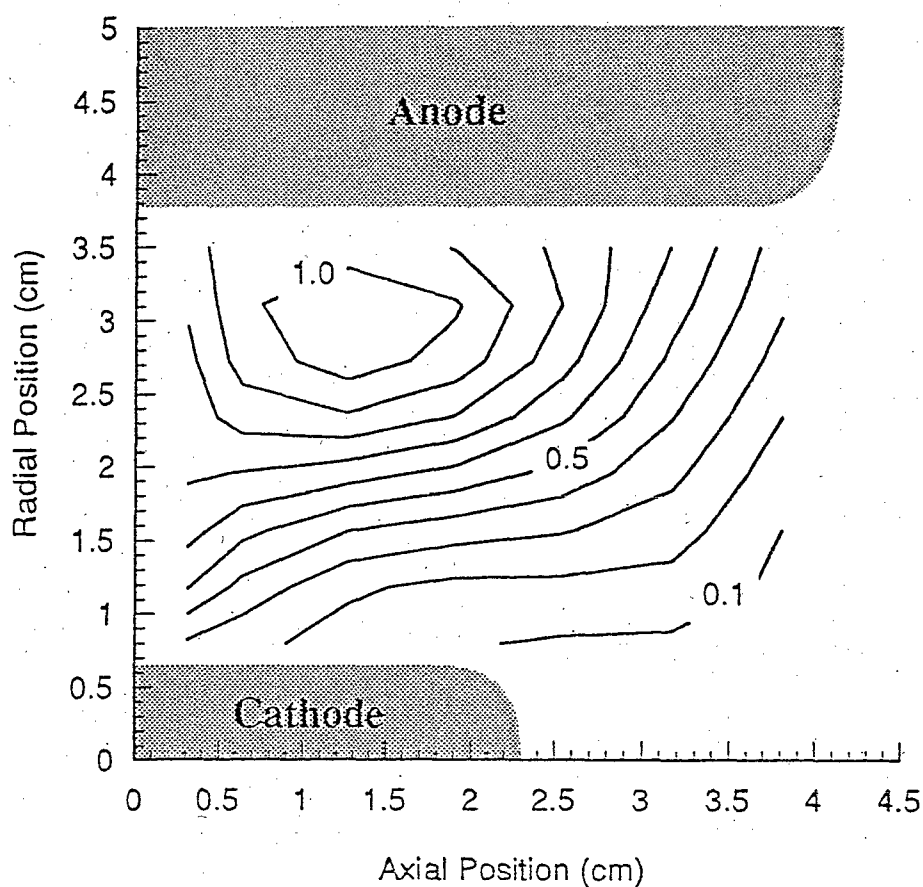


Fig. 5: The enclosed current contours in the experimental MPD thruster operating at 4.4 kA and 0.5 g/sec argon.

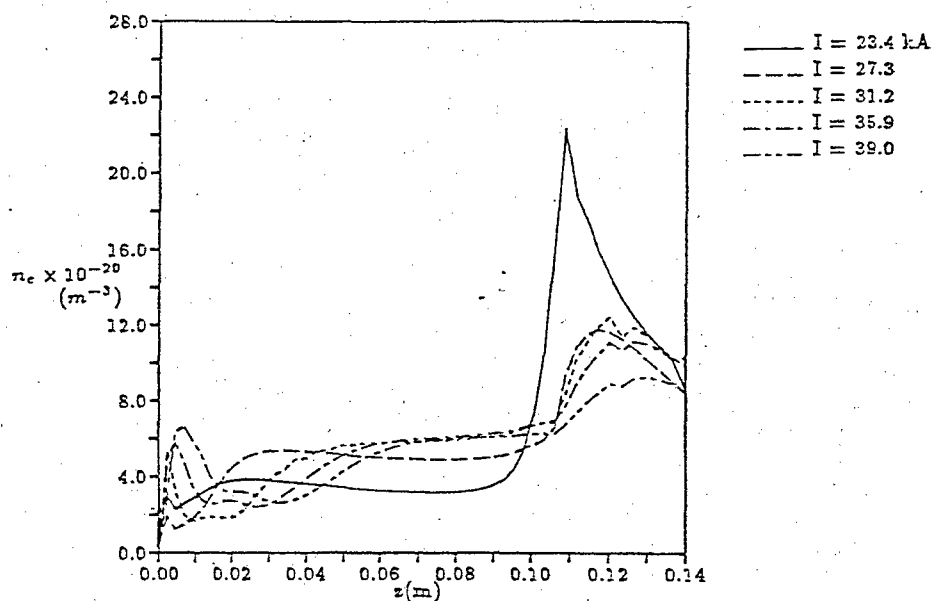


Fig. 6: Model predictions for the electron number density, 1.6 mm from the anode, for the CAC thruster operating at 4 g/sec argon and various current levels.

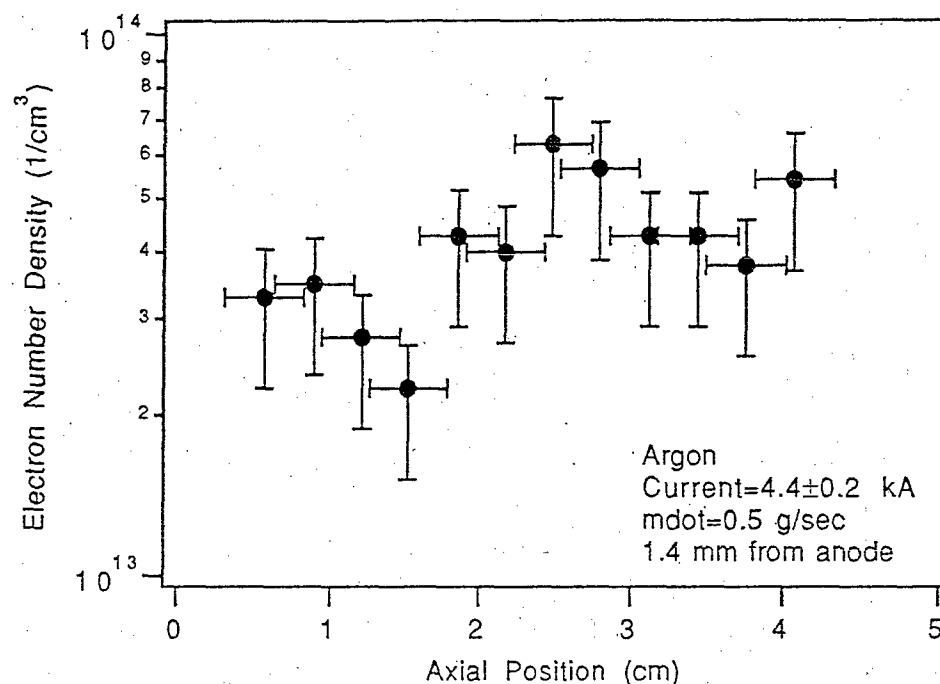


Fig. 7: An axial profile of the measured electron number density near the anode.

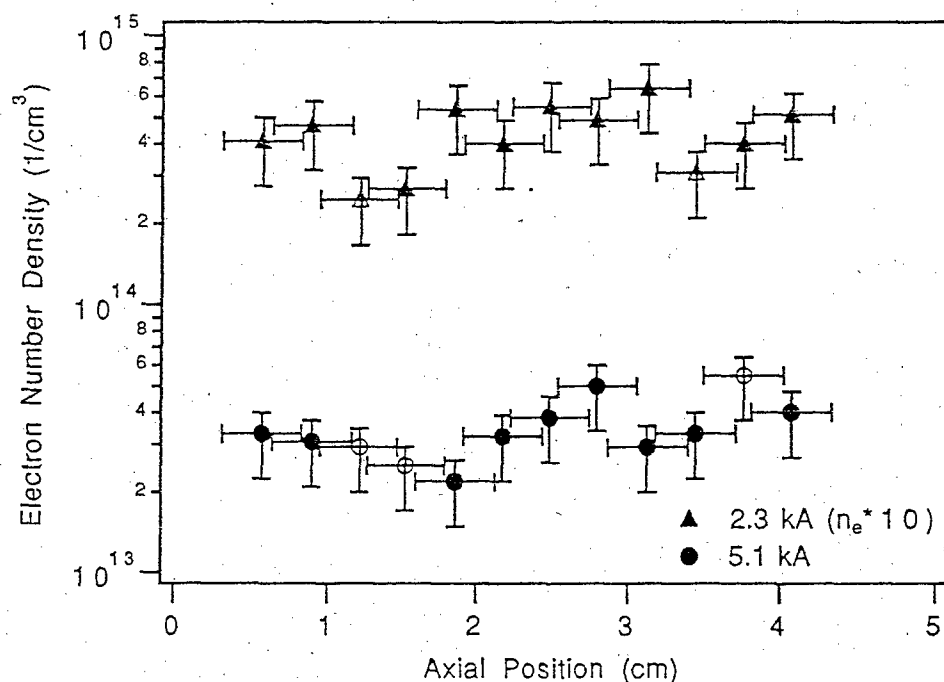


Fig. 8: Axial profiles of the measured electron number density, 1.4 mm from the anode, at 2.3 and 5.1 kA. The open symbols correspond to the location of the peaks in T_e . (0.5 g/sec argon)

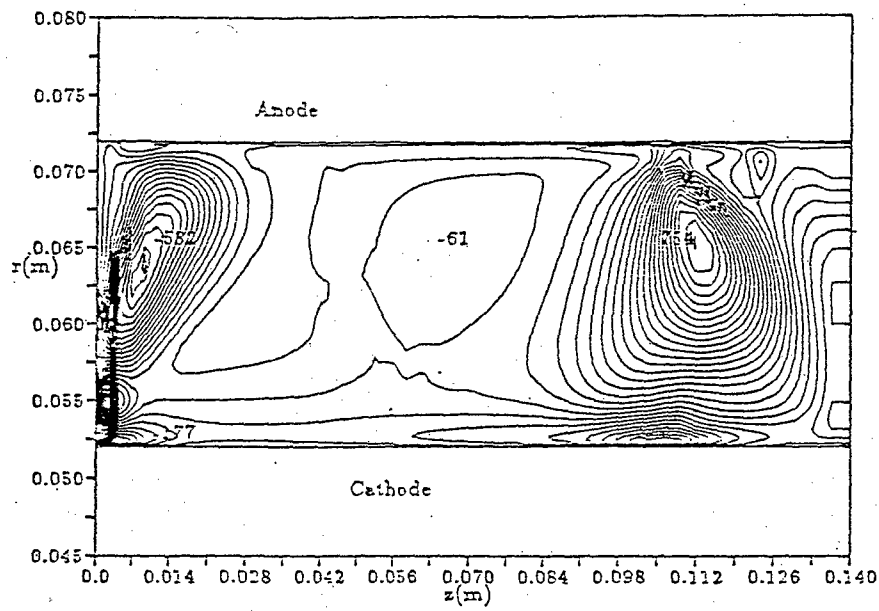


Fig. 9: Model predictions of the radial velocity contours inside the CAC thruster operating at 31.2 kA, 4 g/sec argon.

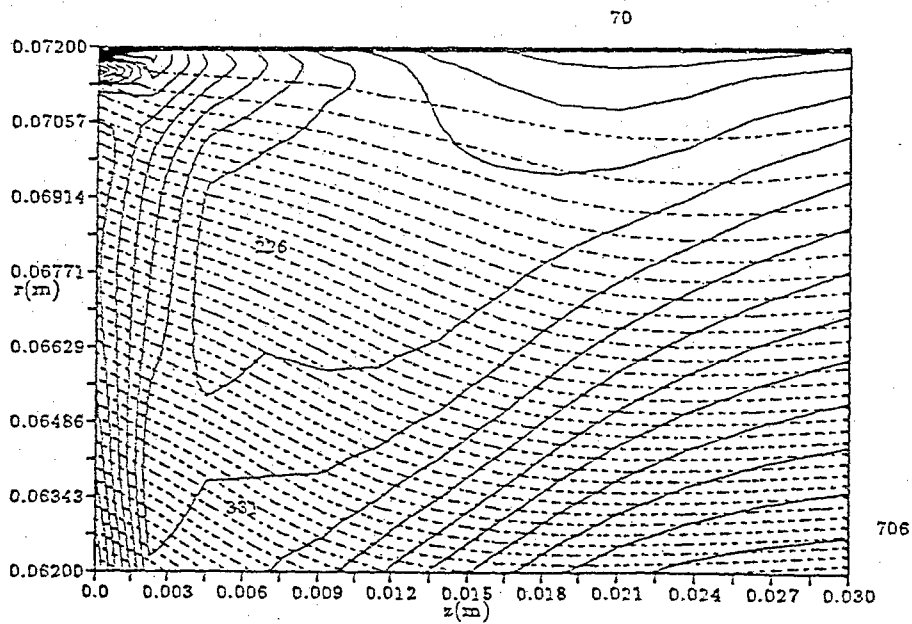


Fig. 10: Streamlines and pressure contours, within 3 cm of the inlet, predicted by the model for the CAC thruster operating at 31.2 kA, 4 g/sec argon.